

Adsorption-Driven Photocatalytic Activity of Mesoporous Titanium Dioxide

Yasuhiro Shiraishi,* Naoya Saito, and Takayuki Hirai

Research Center for Solar Energy Chemistry, and Division of Chemical Engineering, Graduate School of Engineering Science, Osaka University, Toyonaka 560-8531, Japan

Received May 18, 2005; E-mail: shiraish@cheng.es.osaka-u.ac.jp

Development of highly selective methods for photochemical organic synthesis, driven by a heterogeneous catalyst, is one of the biggest challenges in chemistry.¹ Much investigation has been made based on systems using a semiconductor, titanium dioxide (TiO₂).² In most cases, photocatalytic reactions on TiO₂ proceed via the following steps: (i) generation of electron-positive hole pairs by an absorption of supra-band gap photons; (ii) production of hydroxyl radicals (•OH) via reaction of the hole with surface –OH groups or adsorbed H₂O molecules; and (iii) oxidation of substrates by •OH. However, oxidation by •OH is nonselective, resulting in insufficient product selectivity. Recently, two innovative methods were proposed for improvement of catalytic selectivity on TiO₂: (i) creation of molecular recognition site (β -cyclodextrin) for preferential decomposition of targeted substrate;³ and (ii) creation of nonsemiconducting micropores, leading to selective decomposition of large molecules on an external semiconducting TiO₂ surface.⁴ However, a photocatalytic system based on TiO₂, enabling selective “transformation” of molecules and production of “fine chemicals”, had not been developed.

Our system employs TiO₂ with a mesoporous structure (*m*TiO₂). So far, various *m*TiO₂ with different pore size and surface area have been synthesized by means of (i) surfactant-templating method⁵ and (ii) aggregation method consisting of an aggregation of nanosized TiO₂ particles followed by sintering of the particles.⁶ A few reports revealed that *m*TiO₂, as compared to a conventional nonporous TiO₂ (*n*TiO₂), catalyzes a rapid photodecomposition of some substrates, such as 2,4,6-trichlorophenol,^{5c} *n*-pentane,^{5f,6a,e} and acetone.^{6b,f} These enhanced activities are, however, inspired simply by the high surface area of *m*TiO₂; structural advantage of the mesoporous system is left unexploited. Herein, we report an unprecedented photocatalytic activity of *m*TiO₂ driven by an adsorption degree of molecules onto the catalyst surface, which promotes a preferential conversion of well-adsorbed molecules. We highlight a successful application of this property to selective transformation of a well-adsorbed molecule into a less-adsorbed molecule, labeled as “stick-and-leave” transformation, which enables a transformation of benzene into phenol, one of the most difficult synthetic reactions, with very high selectivity (>80%).

We used five kinds of *m*TiO₂(*x*) [*x* = anatase content (%)] with pores of >3 nm diameter (Table 1), prepared by the above two methods,⁷ and *n*TiO₂(*x*) catalysts for comparison. XRD analysis confirmed that all catalysts consisted of anatase and amorphous phases (Figure S1).⁷ Catalytic conversions were carried out by photoirradiation ($\lambda > 320$ nm) to a buffered aqueous solution (pH 7; 10 mL) containing respective substrate (20 μ mol) and catalyst (10 mg).⁷ The degree of substrate adsorption onto the catalyst was defined as the distribution ratio, *D*, based on the adsorption test.⁸

Figure 1 shows a relationship between *D* and conversion of 15 kinds of phenol and phenoxyacetic acid derivatives (1–15), where reactions of all of the substrates are initiated by •OH.⁹ On *n*TiO₂ (Figure 1A), practically no relationship is observed, although substrate conversions tend to increase with an increase in anatase

content of the catalyst. In contrast, *m*TiO₂(65, 61, 57, 37) demonstrates peculiar relationships (Figure 1B): (i) conversions of substrates with low *D* value (<0.05) are nearly zero; and (ii) conversions of substrates with higher *D* value are obviously higher. None of the properties of catalysts [band gap energy (*E*_{bg}), particle size, and surface hydrophobicity (monolayer adsorption capacity of H₂O, *q*_{H2O})] or substrates [oxidation potential, HOMO level, and hydrophobicity (log *P*)], which usually affect the catalytic activity of *n*TiO₂,¹⁰ can explain the unusual activity of *m*TiO₂ (Table 1; Table S1⁷), leading to the degree of substrate adsorption as the strong factor.

On *m*TiO₂(0), conversion for all tested substrates is nearly zero (Figure 1B), as is also observed on *n*TiO₂(0) (Figure 1A). This is because the photoformed electron and positive hole recombine easily on the amorphous surface.^{10a} AggTiO₂(36),^{6c} which was prepared by aggregation method without calcination and which contains high surface area but almost no mesopores (Figure S2⁷), does not show such adsorption-dependent profile (Figure 1A). Calcination of aggTiO₂ leads to a formation of mesopores due to sintering of the particles, along with an increase in anatase content [*m*TiO₂(57)]^{6c} (Figure S2⁷). The use of *m*TiO₂(57) shows an adsorption-dependent profile (Figure 1B), as do *m*TiO₂(65, 61, 37). These findings strongly suggest that the unusual activity of *m*TiO₂ is triggered by a combination of anatase phase and mesopores on the catalyst. It is noted that *m*TiO₂(57), prepared by aggregation method, has more disordered mesostructure than *m*TiO₂(65, 61, 37)⁶ (Figure S1⁷), indicating that a well-ordered porous system is not necessary for the catalytic activity.

ESR spin-trap technique with α -phenyl-*N*-tert-butyl nitron (PBN) was used to clarify the catalytic mechanism on *m*TiO₂ involving •OH.⁷ UV irradiation to *m*TiO₂ containing anatase phase, when suspended in aqueous PBN solution, gives PBN–•OH spin adduct signals, as also for *n*TiO₂(100) (Figure 2A).¹¹ ESR silence with *n*TiO₂(0) and *m*TiO₂(0) (Figure 2A) indicates that •OH is formed mainly on the anatase phase.^{10a} Considering the large internal surface area of *m*TiO₂, most of anatase phase should exist within the mesopores; meaning, •OH production on *m*TiO₂ must occur mainly on the internal surface. Meanwhile, substrate adsorption onto *m*TiO₂ should take place mainly within the pores of high surface area. Therefore, the concentrations of substrates with higher *D* value inside the pore are expected to be higher than those with lower *D* value; the substrates with higher value may be attacked effectively by the •OH inside the pore.

PBN is scarcely adsorbed on all of the catalysts (*D* = 0). On the basis of the above assumption, the PBN concentration within the pore is expected to be lower than that in bulk solution. Figure 2B shows the PBN–•OH intensity, obtained by double integration of the lowest magnetic field signal of the PBN–•OH (Figure 2A). The intensity on *n*TiO₂ increases linearly with an increase in anatase content, as expected. However, the intensity on *m*TiO₂(65) and *m*TiO₂(61) is obviously lower than that on *n*TiO₂(58), although anatase content is higher. As reported,¹² •OH is trapped on the TiO₂

Table 1. Properties of Catalysts

catalyst	anatase (%) ^a	A_{BET} (m^2g^{-1}) ^b	A_{ext} (m^2g^{-1}) ^c	D_p (nm) ^d	E_{bg} (eV) ^e	particle size (μm) ^f	$Q_{\text{H}_2\text{O}}$ (molecules nm^{-2}) ^g	synthesis
$m\text{TiO}_2(65)$	65	171	25	4.6	3.01	2.3	8.0	<i>h</i>
$m\text{TiO}_2(61)$	61	308	33	3.2	3.06	2.2	4.8	<i>h</i>
$m\text{TiO}_2(57)$	57	164	29	3.0	3.03	2.1	8.1	<i>i</i>
$m\text{TiO}_2(37)$	37	161	17	3.4	3.08	1.8	6.7	<i>h</i>
$m\text{TiO}_2(0)$	0	135	38	6.8	2.89	1.9	8.4	<i>h</i>
$n\text{TiO}_2(100)$	>99	50	48		3.08	7.0	6.6	<i>j</i>
$n\text{TiO}_2(58)$	58	81	76		3.08	5.6	7.7	<i>j</i>
$n\text{TiO}_2(0)$	0	127	112		3.10	1.9	10.4	
$\text{aggTiO}_2(36)$	36	297	44		3.01	3.3	12.9	<i>k</i>

^a Measured according to literature procedure.^{10a} ^b BET surface area. ^c External surface area determined by the *t*-plot volumetric measurements with N_2 . ^d Determined by the DH method. ^e Measured by a plot of the Kubelka–Munk function versus the energy of light absorbed. ^f Determined by a laser scattering technique. ^g Monolayer adsorption capacity of H_2O , as determined by dividing the amount of H_2O adsorbed on the catalyst by A_{BET} . ^h By surfactant templating method.^{5e,7} ⁱ By aggregation method.^{6c,7} ^j By calcination of $n\text{TiO}_2(0)$.⁷ ^k By aggregation method without calcination.^{6c,7}

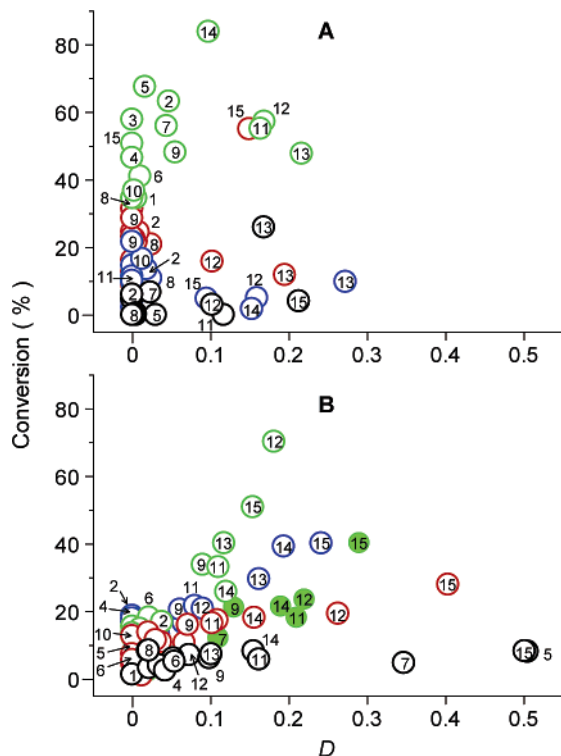


Figure 1. Relationship between the distribution ratio, D , and substrate conversion (0.5 h) on (A) $n\text{TiO}_2(x)$ (green open circle, $x = 100$; red open circle, 58; black open circle, 0) and $\text{aggTiO}_2(36)$ (blue open circle) and (B) $m\text{TiO}_2(x)$ (blue open circle, $x = 65$; green open circle, 61; solid green circle, 57; red open circle, 37; black open circle, 0). Substrates used are denoted as numbers in the figure: 1, phenol; 2, 2,4,6-trichlorophenol; 3, chlorohydroquinone; 4, 2,4-dichlorophenol; 5, 3-chlorophenol; 6, 4-chlorophenol; 7, 2-chlorophenol; 8, benzyl alcohol; 9, 2,4-dichlorophenoxyacetic acid; 10, *p*-cresol; 11, phenoxyacetic acid; 12, 1,2,4-trihydroxybenzene; 13, 1,3,5-trihydroxybenzene; 14, 4-chlorophenoxyacetic acid; 15, 2,6-bis(hydroxymethyl)-*p*-cresol. Detailed data for D and conversion of substrates on $m\text{TiO}_2$ are shown in Table S1.7.

surface and is converted to an inactive surface $-\text{OH}$ group in a near-diffusion-controlled rate. Calculation based on a simple cylindrical model (see discussion⁷ in the Supporting Information) reveals that diffusion distance of $\bullet\text{OH}$ formed inside the mesopore on $m\text{TiO}_2$ is 1.3–2.4 nm, which is smaller than the pore diameter of $m\text{TiO}_2$ (Table 1), suggesting that $\bullet\text{OH}$ formed inside the pore is deactivated rapidly and, hence, scarcely diffuses out of the pores. These findings clearly support the above assumption: on $m\text{TiO}_2$, most of PBN exists out of the pores and cannot react sufficiently with $\bullet\text{OH}$ formed inside the pore. In contrast, on $n\text{TiO}_2$, PBN reacts easily with $\bullet\text{OH}$ formed on the external surface facing the bulk

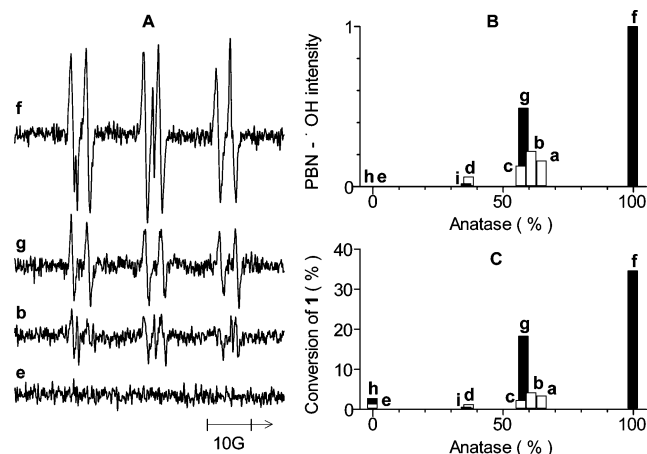
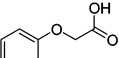
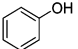
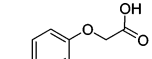
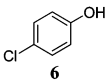
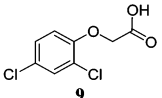
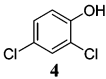
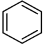
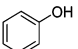


Figure 2. (A) ESR spectra of PBN- $\bullet\text{OH}$ spin adduct obtained by photoirradiation to a catalyst-suspended aqueous PBN solution. (B) The PBN- $\bullet\text{OH}$ intensity obtained by double integration of the lowest magnetic field signal of the adduct, where the intensity obtained with $n\text{TiO}_2(100)$ is set as 1. (C) Photoconversion (0.5 h) of phenol (**1**) on respective catalyst as a function of anatase content of the catalyst. The catalysts are: (a) $m\text{TiO}_2$ -(65), (b) $m\text{TiO}_2(61)$, (c) $m\text{TiO}_2(57)$, (d) $m\text{TiO}_2(37)$, (e) $m\text{TiO}_2(0)$, (f) $n\text{TiO}_2$ -(100), (g) $n\text{TiO}_2(58)$, (h) $n\text{TiO}_2(0)$, and (i) $\text{aggTiO}_2(36)$.

solution, thus leading to higher PBN- $\bullet\text{OH}$ intensity (Figure 2B). When conversion of **1**, which is scarcely adsorbed on all of the catalysts ($D = 0$) as also for PBN, is plotted against anatase content of the catalyst (Figure 2C), the obtained profile is similar to that of the PBN- $\bullet\text{OH}$ intensity (Figure 2B). This fact explains the full picture of the adsorption-driven activity of $m\text{TiO}_2$ (Figure 1B): a well-adsorbed molecule (high D) diffuses well inside the pores and reacts easily with $\bullet\text{OH}$, whereas a less-adsorbed molecule (low D) scarcely enters the pores and cannot react with $\bullet\text{OH}$. As shown in Figure 1A, on $\text{aggTiO}_2(36)$, no adsorption dependence is observed, and conversions are lower than those on $m\text{TiO}_2(37)$. In addition, $\text{aggTiO}_2(36)$ shows rather lower PBN- $\bullet\text{OH}$ intensity and conversion of **1** than does $m\text{TiO}_2(37)$ (Figure 2). This may be because substrates cannot diffuse smoothly inside the narrow micropores on aggTiO_2 , indicating that the presence of “mesopores”, which allow a smooth diffusion of molecules, is necessary for the adsorption-driven activity.¹³

The unique activity of $m\text{TiO}_2$ is applicable to a selective transformation of several molecules (Table 2). Photoirradiation of **11** on $n\text{TiO}_2$ gives rise to **1** as an initial product (runs 1, 2) via $\bullet\text{OH}$ -induced ether bond cleavage,¹⁴ but the selectivity is not so high (<35%) because sequential oxidation of **1** by $\bullet\text{OH}$ occurs on $n\text{TiO}_2$.¹⁵ However, on $m\text{TiO}_2$ (run 3), **1** is obtained with more than twice the selectivity (72%). This is because **1** is scarcely adsorbed on $m\text{TiO}_2$ ($D = 0$) and, hence, suppresses the sequential oxidation

Table 2. Photocatalytic Transformation of Various Substrates^a

run	catalyst	reactant	<i>D</i>	conv (%)	product	<i>D</i>	yield (%)	select (%)
1	<i>n</i> TiO ₂ (100)		0.17	90		0.01	39	35
2	<i>n</i> TiO ₂ (58)		0	82		0	28	34
3	<i>m</i> TiO ₂ (61)	11	0.11	89	1	0	61	72
4	<i>n</i> TiO ₂ (100)		0.10	91		0.01	16	18
5	<i>n</i> TiO ₂ (58)		0	87		0	11	13
6	<i>m</i> TiO ₂ (61)	14	0.12	90	6	0	65	72
7	<i>n</i> TiO ₂ (100)		0.05	60		0	26	23
8	<i>n</i> TiO ₂ (58)		0	71		0	12	17
9	<i>m</i> TiO ₂ (61)	9	0.09	84	4	0	75	89
10	<i>n</i> TiO ₂ (100)		0.24	26		0.01	2	8
11	<i>n</i> TiO ₂ (58)		0.28	16		0	1	6
12	<i>m</i> TiO ₂ (61)		0.64	23		0	19	83
13 ^b	<i>m</i> TiO ₂ (61)	16	0.64	42	1	0	34	81
14 ^c	<i>m</i> TiO ₂ (61)		0.64	10		0	8	80

^a Reaction conditions were: reactants, 20 μmol; photoirradiation time, 2 h; catalyst, 10 mg; buffered (pH 7) aqueous solution, 10 mL; temperature, 313 K. ^b Photoirradiation time, 6 h. ^c Reactant, 0.5 mmol (which is not fully dissolved in the aqueous solution).

of **1**. For chloro-substituted phenoxyacetic acids (**14** and **9**) on *n*TiO₂ (runs 4, 5 and 7, 8), the initially formed chlorophenols (**6** and **4**) are converted rapidly via substitution of –Cl by –OH to form totally hydroxylated products.^{14,16} However, on *m*TiO₂ (runs 6, 9), the –Cl substitution is suppressed because of low adsorption degree of the chlorophenols (*D* = 0), thus affording them with high selectivity (>72%). These examples clearly demonstrate that the present *m*TiO₂ system promotes a selective transformation of a well-adsorbed molecule into a less-adsorbed molecule, so-labeled stick-and-leave transformation.

The most notable application of the present system is a direct hydroxylation of benzene (**16**) to phenol (**1**). On *n*TiO₂, the initially produced **1** is sequentially oxidized by •OH to form further hydroxylated products (runs 10, 11).¹⁵ On *m*TiO₂, **16** is adsorbed strongly (*D* = 0.64), but **1** is scarcely adsorbed (*D* = 0). The sequential hydroxylation of **1** is therefore suppressed, thus affording **1** with very high selectivity (>80%) (runs 12, 13). The 0.5 mmol scale experiment is also successful for the production of **1** (run 14). To the best of our knowledge, this is a photocatalytic system achieving the highest selectivity of **1** among those which have been proposed so far (<21% selectivity) (Table S2⁷). As well-known, the synthesis of **1** from **16** is currently carried out industrially via a multistep cumene process, but the process suffers from low selectivity, high energy consumption, and formation of a large quantity of byproducts. So far, various catalytic processes have been proposed as alternatives, where some of them achieve higher selectivity of **1** than the system proposed here, but they require expensive oxidants, noble metals, or severe reaction conditions (Table S3).⁷ The system proposed here exhibits significant advantages: (i) additive-free, (ii) cheap source of oxidant (H₂O), and (iii) mild reaction condition (room temperature). Photocatalytic phenol synthesis may be realized by applying the basic concept proposed here, and the present system has a potential to enable this and other photocatalytic organic synthesis in an economically and environmentally friendly way.

Acknowledgment. This work is supported by the Grant-in-Aids for Scientific Research (No. 15360430) and on Priority Areas “Fundamental Science and Technology of Photofunctional Interfaces (417)” (No. 17029037) from the Ministry of Education, Culture, Sports, Science and Technology, Japan (MEXT).

Supporting Information Available: Materials and Methods, Discussion, Tables S1–S4, and Figures S1 and S2. This material is available free of charge via Internet <http://pubs.acs.org>.

References

- (1) Coyle, J. D.; Carless, H. A. C. *Photochemistry in Organic Synthesis*; Royal Society of Chemistry: London, 1986.
- (2) (a) Bard, A. J. *J. Phys. Chem.* **1982**, *86*, 172–177. (b) Fox, M. A.; Dulay, M. T. *Chem. Rev.* **1993**, *93*, 341–357. (c) Fox, M. A. *Acc. Chem. Res.* **1983**, *16*, 314–321. (d) Maldotti, A.; Molinari, A.; Amadelli, R. *Chem. Rev.* **2002**, *102*, 3811–3836. (e) Mills, A.; Le Hunte, S. J. *Photochem. Photobiol. A: Chem.* **1997**, *108*, 1–35. (f) Fujishima, A.; Rao, T. N.; Tryk, D. A. J. *Photochem. Photobiol. C: Photochem. Rev.* **2000**, *1*, 1–21.
- (3) Ghosh-Mukerji, S.; Haick, H.; Schwartzman, M.; Paz, Y. *J. Am. Chem. Soc.* **2001**, *123*, 10776–10777.
- (4) (a) Calza, P.; Pazé, C.; Pelizzetti, E.; Zecchina, A. *Chem. Commun.* **2001**, 2031–2032. (b) Llabrés i Xamena, F. X.; Calza, P.; Lamberti, C.; Prestipino, C.; Damin, A.; Bordiga, S.; Pelizzetti, E.; Zecchina, A. *J. Am. Chem. Soc.* **2003**, *125*, 2264–2271.
- (5) (a) Antonelli, D. M.; Ying, J. Y. *Angew. Chem., Int. Ed. Engl.* **1995**, *34*, 2014–2017. (b) He, X.; Antonelli, D. M. *Angew. Chem., Int. Ed.* **2002**, *41*, 214–229. (c) Dai, Q.; He, N.; Guo, Y.; Yuan, C. *Chem. Lett.* **1998**, 1113–1114. (d) Yang, P.; Zhao, D.; Margoless, D. I.; Chmelka, B. F.; Stucky, G. D. *Nature* **1998**, *396*, 152–155. (e) Tian, B.; Yang, H.; Liu, X.; Xie, S.; Yu, C.; Fan, J.; Tu, B.; Zhao, D. *Chem. Commun.* **2002**, 1824–1825. (f) Zhang, L.; Yu, J. C. *Chem. Commun.* **2003**, 2078–2079. (g) Peng, Z.; Shi, Z.; Liu, M. *Chem. Commun.* **2000**, 2125–2126.
- (6) (a) Yu, J. C.; Zhang, L.; Zheng, Z.; Zhao, J. *Chem. Mater.* **2003**, *15*, 2280–2286. (b) Yu, J. C.; Zhang, L.; Yu, J. *New J. Chem.* **2002**, *26*, 416–420. (c) Uekawa, N.; Suzuki, M.; Ohmiya, T.; Mori, F.; Wu, Y. J.; Kakegawa, K. *J. Mater. Res.* **2003**, *18*, 797–803. (d) Yoo, K.; Choi, H.; Dionysiou, D. D. *Chem. Commun.* **2004**, 2000–2001. (e) Yu, J. C.; Zhang, L.; Yu, J. *Chem. Mater.* **2002**, *14*, 4647–4653. (f) Yu, J.; Yu, J. C.; Leung, M. K.-P.; Ho, W.; Cheng, B.; Zhao, X.; Zhao, J. *J. Catal.* **2003**, *217*, 69–78.
- (7) See Supporting Information.
- (8) $D = (C_0 - C_e)/C_e$, where C_0 denotes the initial concentration of substrate in solution and C_e denotes the equilibrium concentration of the substrate in the solution after stirring with catalyst (313 K; 0.5 h).
- (9) Almost no reaction occurs in the presence of D-mannitol, a typical •OH scavenger (100-fold molar excess based on the substrate).
- (10) (a) Ohtani, B.; Ogawa, Y.; Nishimoto, S.-i. *J. Phys. Chem. B* **1997**, *101*, 3746–3752. (b) Sclafani, A.; Palmisano, L.; Schiavello, M. *J. Phys. Chem.* **1990**, *94*, 829–834. (c) Ohtani, B.; Okugawa, Y.; Nishimoto, S.-i.; Kagiya, T. *J. Phys. Chem.* **1987**, *91*, 3550–3555.
- (11) Janzen, E. G.; Nutter, D. E., Jr.; Davis, E. R.; Blackburn, B. J.; Poyer, J. L.; McCay, P. B. *Can. J. Chem.* **1978**, *56*, 2237–2242.
- (12) Lawless, D.; Serpone, N.; Meisel, D. *J. Phys. Chem.* **1991**, *95*, 5166–5170.
- (13) Catalytic activity of *m*TiO₂ depends on its anatase content and surface area; *m*TiO₂(65) clearly shows higher substrate conversions than *m*TiO₂(37) (Figure 1B). This is because the former contains a higher quantity of anatase phase and hence produces a higher quantity of •OH. *m*TiO₂(61) shows higher substrate conversions than *m*TiO₂(65) (Figure 1B), despite the lower anatase content. This is because the former, having twice larger surface area than the latter (Table 1), has larger anatase surface area.
- (14) Tanaka, K.; Reddy, K. S. N. *Appl. Catal. B* **2002**, *39*, 305–310.
- (15) Hashimoto, K.; Kawai, T.; Sakata, T. *J. Phys. Chem.* **1984**, *88*, 4083–4088.
- (16) Al-Ekabi, H.; Serpone, N.; Pelizzetti, E.; Minero, C.; Fox, M. A.; Draper, R. B. *Langmuir* **1989**, *5*, 250–255.

JA053265S